

Notes on
Defect-Driven Spatial Temporal Chaos

Nicholas B. Tuffiaro
Physics Department
Bryn Mawr College,
Bryn Mawr PA 19010 USA
BITNET: NBT@BRYNMAWR

27 March 1988

Abstract:

A somewhat bs stream of consciousness account of current experiments on capillary ripples with gradious generalizations to other systems exhibiting spatial/temporal chaos.

Defect-Driven Spatial Temporal Chaos

I. Introduction

The notion of a 'phase transition' has broadened in the last few decades, and at the same time, it has grown to encompass quite an expanse of physical phenomena. At least four rough categories of phase transitions can be identified (Anderson, Basic Notions of Condensed Matter Physics):

<u>Example.</u>	<u>Symmetry.</u>	<u>Change.</u>
condensed matter/ solid state.	local homogeneity & isotropy broken.	complete change of microscopic properties.
cosmological/big bang.	nonlinearities cause instability: driven by small fluctuations.	little change in local properties.
laser.	local microscopic symmetry broken by external pumping.	coherence, but no regularity, rigidity.
Kondo effect.	No broken symmetry.	continuous transition to qualitatively different behavior.

As the use of 'phase transition analogies' has broadened to cross-fertilize many disciplines from cosmology to elementary particles; the notion of a phase transition itself has blurred. As the Kondo effect illustrates; the notion of a phase transition is not even always associated with a broken symmetry.

It seems that the only reasonable definition of a phase transition is the rather vacuous statement that a phase transition occurs when a

measurable quantity of a physical system undergoes an abrupt change. Given such a change, phase transitions are usually divided into two cases: *continuous* and *discontinuous*. First-order transitions are discontinuous and all continuous transitions are loosely called second order. Continuous (2nd order) transitions can also be divided into two types: *instability transitions* and *nucleation transitions* (Fluctuations, Instabilities, and Phase Transitions, ed. T. Riske).

In this paper we will be concerned with nucleation type 2nd order phase transitions. In particular, we will argue that a qualitative change in the spontaneous pattern formation in far from equilibrium systems (eg. multimode lasers, Bernard-Marangoni flow, neumatic-shear flow, capillary ripples) can be understood as a defect-mediated phase transition (Nelson, Phase Transition and Critical Phenomena, vol. 7), i.e., as a one or two stage melting process. The basic scenerio we invision is this; a far from equilibrium system is driven until it forms a structure breaking the homgenity and isotropy of the problem. In a fluid problem these structures could be Benard rolls or cells; in a laser this structure could be the transverse field intensity across the cavity (a checkered optical Zebra if you like). As the driving term of the system is futher increased the nonlinearities in the system cause some local or global modulation of these structures, leading, in effect, to defects in the self organized structures (these are called "auto-structures" in the soviet liteature). The structures now lose some (but perhaps not all) of their order due to these defects. The order can be lost in one or more stages. Following Ocelli et. al. (J. Physique Lett. 49 (1983) L-567) we propose the use of 'multiple point' correlation functions taylored to each problem to quantify this loss of order. At the end we will consider a specific application of these ideas to current experiments on capillary waves as well as suggest their possible application to transverse instabilities in multimode lasers.

However, we would like to stress that the basic methodology should be applicable to the study of pattern formation in many far from equilibrium systems. Also these ideas could be the basis for a theoretical research program in spatial-temporal chaos. The idea is to attempt to classify the types of defects that can arise in patterns (this could be done, for instance, from a qualitative analysis of modulations that arise in generalized amplitude equations e.g. Landau-Ginzburg equation) in far from equilibrium systems. The guess is that the analysis of different types of defects may give rise to information about the type of phase transitions the system can exhibit. In fact, this is exactly what has been accomplished for the analysis of melting transitions as we will discuss shortly. In this paper we will show that for some experimental systems the patterns and their defects can be analyzed experimentally. The connection (if any) between the type (topologically ?) of defects and different types of phase transitions has yet to be explored.

II. Defect-mediated phase transitions.

During the last decade Nelson and others (Nelson, *Phase Transitions and Critical Phenomena*, vol. 7) have devised a theory of melting where the melting process occurs because of the formation of dislocation pairs at sufficiently high temperatures (Nelson & Halperin, *Phys. Rev. B* **19** (5) 2457). The theory is particularly useful for two-dimensional systems, where the theory predicts the existence of a two-stage melting process; the first stage of which destroys translational order while the second stage destroys orientational order. A recent experimental confirmation of the theory is provided by Murray and Van Winkle (*Phys. Rev. Lett.* **58** (12) 1200) who observe this two-stage melting transition in a two-dimensional colloidal suspension of highly charged, submicron-sized spheres in water using optical microscopy and digital imaging.

$$\rho_{\vec{G}}(\vec{r}) = e^{i\vec{G} \cdot \vec{r}}$$

is a reciprocal lattice vector and \vec{r} particle position. For two dimensional solid, quite general arguments show that no long range order

However for a 2-D solid the translational correlation function is like a power law

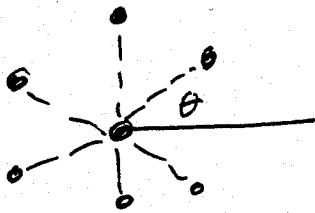
$$G(r) \sim (1/r)^\eta$$

is related to the elastic coefficient (Lame coefficient) of a 2-D solid in this situation we speak of quasi-long range order.

Originally suggested by Halperin and Nelson (Phys. Rev B 41, 121; 1978)) a notion of orientational order can also be defined by the order parameter

$$\psi_b(\vec{r}) = e^{6i\theta(\vec{r})}$$

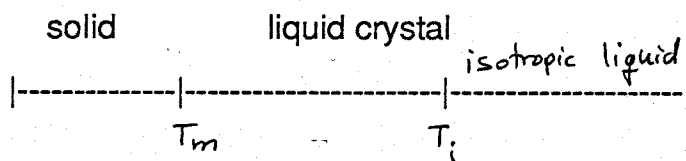
below,



angle made by the line joining two neighboring atoms relative to reference axis, while \vec{r} locates the mid-point of the bond. By 'bond', not necessarily mean a chemical bond, but merely a relation between nearest neighbors, based, possibly on a geometric construction like a Voronoi polygon (Collins, Phase Transitions and Critical Phenomena). The quantity $e^{6i\theta}$ is appropriate for studying triangular lattices, $e^{4i\theta}$ is the order parameter for square lattices. Thus, the correct orientational

the orientational correlation function can be computed for a lattice (a model of a solid) or for a net (a random collection of points modeling a liquid). Briefly the construction is simply the Wigner-Seitz construction of solid state physics where one draws perpendicular bisectors between line segments connecting nearest neighbors. This construction provides a unique ^{partition} tiling of the plane (c.f. Loeb, Space Structures, chapter 13).

The notions of orientational and translational order are not exclusive. Certain types of defects in a lattice can destroy one or both of these correlations. Other types of defects will only destroy one type of order, for instance, a stack fault will destroy translational order but not orientational order. In fact, the existence of different types of order suggests the possibility of an phase intermediate between a liquid and a solid. In a melting process Nelson and Halperin show that this intermediate 'liquid crystal' phase can indeed exist. They call this new phase 'hexatic' or 'tetratic' if the phase exhibits sixfold or fourfold symmetry respectively. In fact, they showed that a two-stage melting process could exist where:



	<u>translational corr.</u>	<u>orientational corr.</u>
solid	algebraic decay (quasi long-range order)	constant (long range order)
liquid crystal	exp. decay	algebraic decay
liquid	exp. decay	exp. decay

the melting process exhibits three phases; a solid phase, a liquid crystal phase, and an isotropic liquid phase with the correlation function characteristics given above.

In practice one calculates the translational correlation function

$$G_T(\vec{r}) = \langle \rho_{\vec{G}}^*(\vec{r}) \rho_{\vec{G}}(\vec{0}) \rangle$$

and the orientational correlation function

$$G_O(\vec{r}) = \langle \psi_{\vec{G}}^*(\vec{r}) \psi_{\vec{G}}(\vec{0}) \rangle$$

to distinguish the different phases. G_T is a measure of the departure of each atom from the ideal lattice location, while G_O measures the local deviation of each bond angle from its solid configuration; these are not simple spatial correlation functions but actually measure the deviation from some predetermined structure. They are perhaps better called pattern recognition functions since they measure the deviation from a translational or orientational pattern. They are also typically not continuous, but are rather summed over a discrete number of sites in the problem.

III. Methodology.

Ocelli et. al. (J. Physique Lett. **44** (1983) L-567) have successfully calculated the orientational and translational correlation functions from experimental data from Bernard-Manangoni flow and nematic-shear flow. Also, Murray and Van Winkle (Phys. Rev Lett. **58** (12) 1200 (1987)) have determined these functions for an experimental melting problem. We are currently trying to apply these methods for patterns seen in capillary ripples to be described in the next section. Before we see the details I would like to point out that there is a general methodology to these experimental techniques.

First, a collection of patterns are identified in the system such as rolls or cells. Second, these patterns are given an 'outline', i.e. a pictorial description based on a 1-bit quantization of the essential features. Third, deviations within the pattern are measured by appropriate correlation functions. These deviations typically arise from defects (dynamical

instabilities) in the pattern. Several different correlation functions can be employed, each measuring some different aspect of the problem such as translational or orientational order. Lastly, different states of the pattern (phase transitions) can be identified by quantitative changes in the correlation functions. We next discuss how this program can be implemented for capillary wave turbulence.

IV. Capillary Ripples

Capillary ripples can be generated on the surface of a liquid when the liquid is forced to vibrate in the vertical direction. The system can be viewed as a parametric fluid oscillator since by shaking the liquid up and down, we are, in effect modulating the gravitational acceleration. We are interested in studying the patterns that form on the surface of the liquid. These patterns will be generated by capillary waves in the frequency range we work in. The basic size of the ripples is determined by the capillary wave dispersion relation

$$\frac{\omega_p}{2} = \left(\frac{\alpha}{\rho} \right)^{1/2} \left(\frac{2\pi}{\lambda} \right)^{3/2}$$

where α is the surface tension, ρ is the density of the fluid and ω_p is the forcing frequency. Our experimental apparatus uses n-butyl alcohol with a forcing frequency of 320 Hz. This gives a capillary wavelength of about 2 mm. Our fluid container is 8cm x 8cm x 1cm, so we study a large aspect ratio (many modes problem) in the deep wave limit. A detailed description of the experimental apparatus is given by Simonelli & Gollub (Rev. Sci. Inst. **59**(2) 286 (1988)). Briefly, the apparatus consists of a square plexiglass container coupled to an industrial shaker undergoing periodic vertical oscillations. The surface of the liquid is visualized by shining a collimated white light beam into the bottom of the cell. The light is

refracted by the deformed liquid at the surface of the cell. The fluid air interface acts as an array of lenses to focus or defocus the light. The light is imaged onto a mylar screen at the top of the cell. This image can be sampled locally with a photodiode or globally with a video camera. Images from the video camera can be saved on a VCR and then digitally processed on a workstation. Typically, only the center of the cell is imaged to minimize the boundary effects.

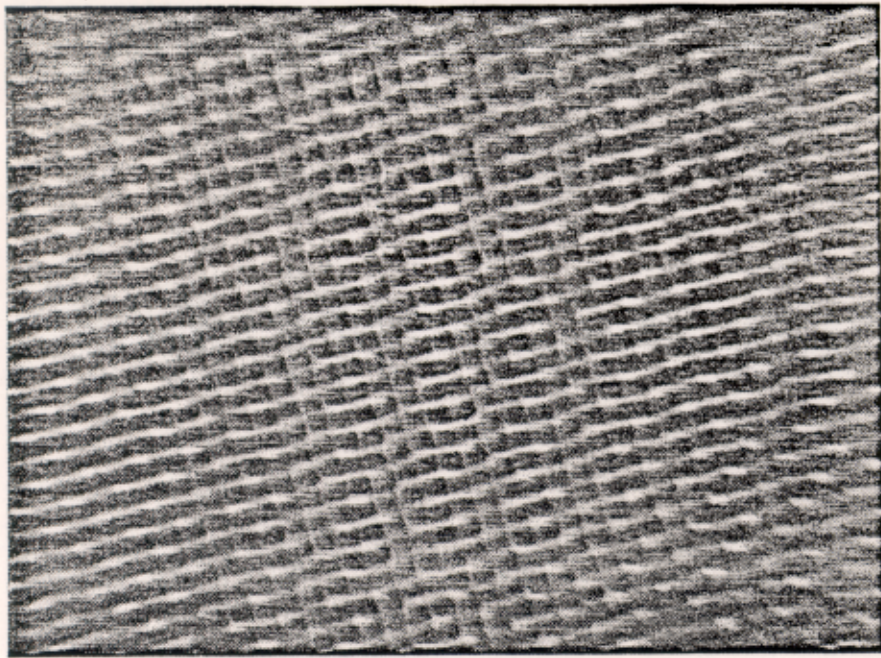
The surface remains flat for small forcing amplitudes. The capillary waves first begin to form at a critical amplitude A_c . As the amplitude is increased further, regions of highly ordered (an almost stationary square lattice) patterns followed by less ordered time dependent patterns are observed.

Three images of the types of patterns are shown in (a), (b), and (c) for increasing excitation amplitude. At an excitation amplitude a bit above A_c , the pattern becomes a highly organized square array with almost time independent behavior. At a higher excitation amplitude the pattern breaks up due to the formation of defects -- which we call 'voids' -- in the lattice. This region is very time dependent. At still a higher amplitude (c), the pattern loses all order and appears to be a net -- a random collection of points possessing only statistical symmetry (Loeb, Space Structures, chapter 4).

In order to quantify these observations a bit the auto-correlation function is measured at the center of the cell with a single photodiode:

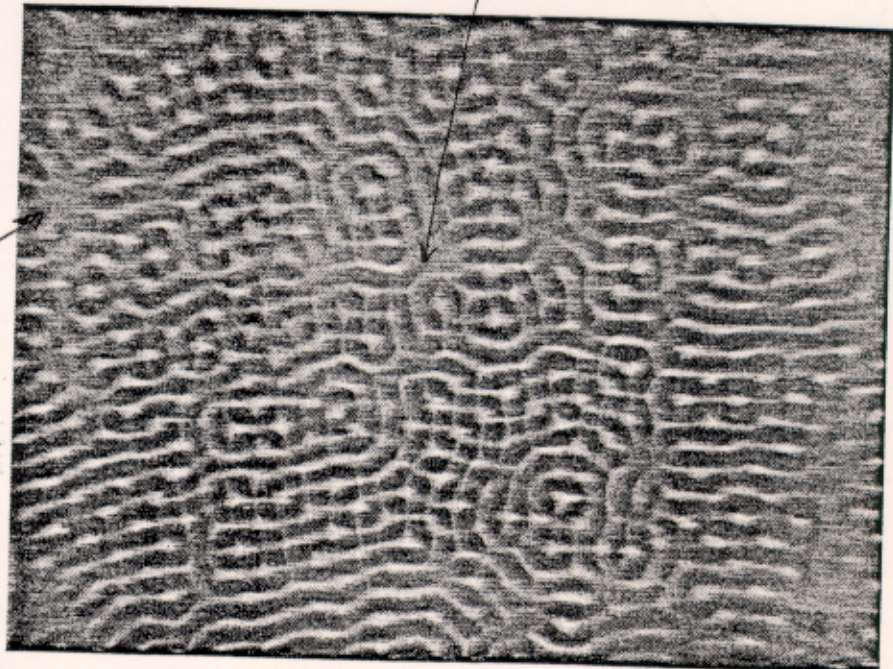
$$g = \langle x(t) x(t+\tau) \rangle$$

where x is the intensity of the image averaged over the diode area 0.5 mm (about one-fourth the capillary wavelength). We calculated the autocorrelation function for each pattern as the excitation amplitude is increased by small increments. For each excitation amplitude, we next calculate the "first half maximum" of the auto correlation function. The

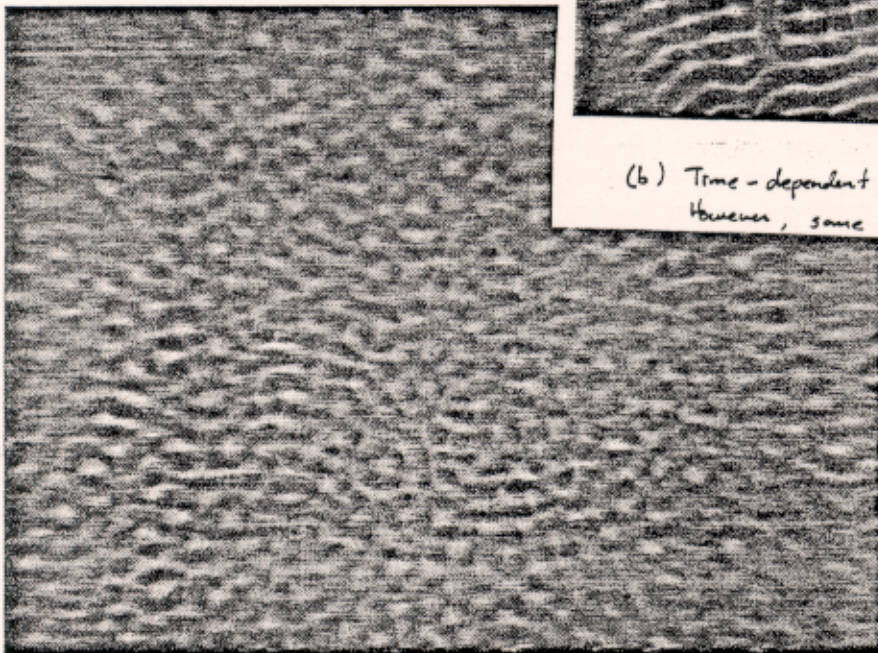


(a) Highly organized square lattice
'almost' stationary regime

315.p



(b) Time-dependent break-up of square lattice.
However, some orientational order remains.



(c) Loss of both translational & orientational order
at high excitation amplitude. 'statistical symmetry'

first half maximum is a rough measure of how long it takes the pattern to move, on average, by one fourth the capillary wavelength. It is a measure of the fastest rearrangement time for the pattern. In the "stationary" regime (the stable square lattice) the first half maximum of the autocorrelation function is simply a measure of the fastest frequency of the system, and is, in fact, one fourth the time it takes the pattern to drift through a distance of the capillary wavelength. Significant correlations can exist in this regime well past the first half maximum.

With the break-up of the square pattern however, the first half maximum is now a good measure of the correlation time of the system, i.e., there do not appear to be any significant correlations beyond the first half maximum. Therefore, in this regime the first half maximum is a measurement of the fastest rearrangement time of the system as well as a good measurement of the correlation time.

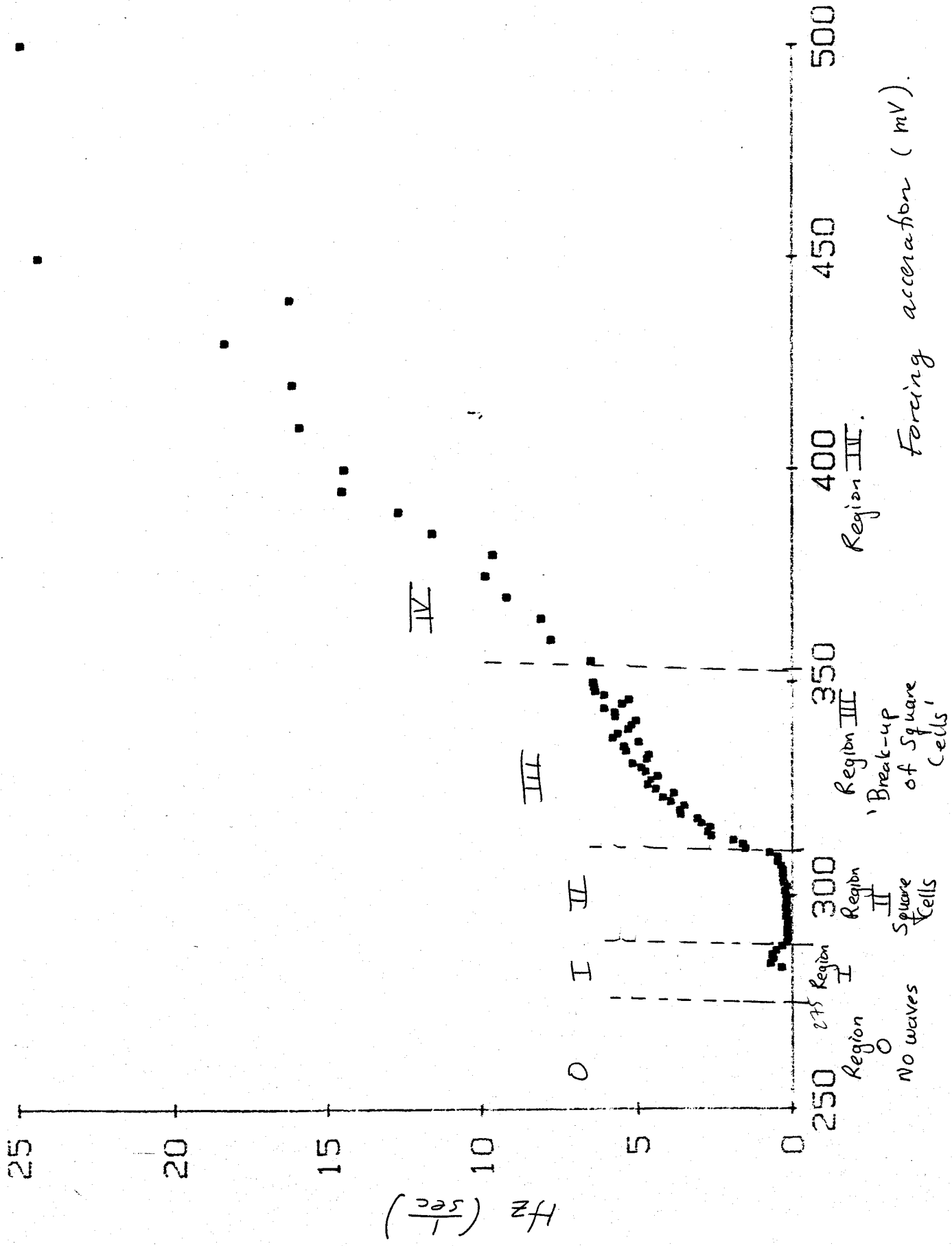
The magnitude of the autocorrelation first half maximum (ACF) vs. the excitation acceleration (in millivolts) is shown in the accompanying plot. This ACF allows us to distinguish four regions as labeled on the plot.

Region 0. No capillary waves, flat surface.

Region I. Pre-formation of square cells. This region can show periodic behavior of a single wave front, quasi-periodic motion of two perpendicular wave fronts presumably interacting linearly; spatial-temporal intermittency between square pattern and more complicated stuff.

Region II. Square pattern. No spatial-temporal intermittency over several minutes. Only real dynamics is the drifting of this pattern. The pattern is orientationally stable, remaining always at one orientation for the whole pattern. The square pattern forms at about the center third of the cell,

1/autocorrhalfmax



initially growing in size, and then decreasing with the onset of the instability. We believe that it does not cover the whole cell because of a nonuniformity in the local acceleration. The ACF is pretty much linear with a slight increase in frequency, i.e., the drift velocity slowly increases with the excitation amplitude. This region is easily identified by eye, or with the ACF. Also modulations of intensity which enter this region appear to be 'damped out' by the lattice. Similar behavior is observed in PDE's and coupled map models of spatial temporal chaos. This is the so-called "stationary" regime of Rabinovich et. al. The first noticeable instability in this regime is the small oscillations of the peaks, this is seen as a jitter on the time series plots, and is the first hint of the onset of an instability.

Region III. Onset of instability. A clear threshold is given by the ACF plot showing a significant increase of the voids causing a marked time dependence. The ACF is approximately square root in this regime. The motion at the onset also becomes orientationally unstable, the square pattern swings back and forth. The pattern is disrupted about every four cells by the instability, thus orientational order exists for distances less than four wavelengths. This is in agreement with similar qualitative observations by Russian authors who observe interesting rearrangements of groups of 3 and 4 cells at a time. Spatial-temporal intermittency is also observed. There appears to be a pattern competition between patterns of square and hexagonal symmetry. We conjecture that this is because energy is now entering into a new mode of the problem generating 6 waves instead of 4. The pattern competition occurs at a relatively slow time scale (30 sec). The spacing between voids and their frequency of production increase with the excitation amplitude.

Region IV. Full turbulence. The production of the instability becomes so

frequent that there is no room from one to the next. At this point all order over the length scale greater than the capillary wave length is lost. This is marked by a less clearly defined threshold in the ACF. At this point the ACF is approximately linear again with a significant slope.

It is tempting to interpret the transition from region I to IV as a two-stage melting process since the spatial temporal chaos is driven by defects -- voids. We are currently planning to test this hypothesis by calculating the G_T and G_4 , the translational and four point orientational correlation functions for this experiment. Unlike the melting process described by Nelson, however, the defects occurring in capillary wave turbulence are not local dislocations, but rather longer wavelength phenomenon which we term voids. These voids are probably formed by the transverse intersection of two transverse instabilities of the type described by Ezerkii et. al. (Sov. Phys. JEPT **64** (6), 1228).

V. Conclusion.

Our next step is to calculate G_T and G_4 to test the two-stage melting scenario. The defects driving this melting process are not local dislocations and this must be taken into account in any theoretical description of the problem. The software needed to calculate the orientational and translational correlation functions from experimental data is quite extensive and will be discussed in a future communication. The software, in the construction of the Wigner-Stietz cells, will also allow us to quantitatively study the number and type of defects that arise in capillary wave turbulence (c.f. McTague et. al. in *Ordering in Two Dimensions* ed. Sinha, p147). This will allow us to study quantitatively how defects drive spatial temporal chaos. Similar studies are at least possible in principle for the optical zebra.